Study the Performance of a Dynamic Wall Heat Exchanger Using Computational Fluid Dynamics

Md Mesbah Uddin, Raisa Akhtaruzzaman, Tanvir Ahmed Shanto, and Mohammad Nasim Hasan

***Abstract* — Thermal systems in small devices like cooling electronic chips require efficient technologies with small diameter channels. These systems have laminar flow and disrupted boundary layers, leading to high pressure drop values. To ensure sufficient flow and limit coolant temperature, a possible solution is to dynamically deform one channel wall to mimic pumping and disrupt boundary layers, creating a peristaltic effect, called a dynamic heat exchanger. The aim of the present numerical study is to explore the effects of different operating parameters of the dynamic wall heat exchanger on the heat transfer performance. In our numerical study we varied different operating parameters (amplitude of vibration A, frequency f, minimum gap between upper and lower wall H and pressure difference ΔP) and observed how it affects the performance of the dynamic wall heat exchanger in terms of mass flow rate of coolant (water) and heat transfer coefficient. A crucial finding is that the distribution of isotherms and streamlines is adequate, and heat transfer is significant when the relative amplitude is high. Additionally, this type of wall can generate substantial heat transfer even with minimal externally applied pressure.**

***Keywords* — Dynamic Wall Heat Exchanger, Computational Fluid Dynamics, Heat Transfer, Numerical Analysis.**

I. Introduction

Thermal systems used in miniature devices, such as cooling embedded electronic chips, microelectronics, power stations, heat pumps, and industrial processes in metallurgy, require efficient technologies involving small diameter channels with hydraulic diameters in the millimeter range. These systems mostly exhibit laminar flow, and the boundary layers are not effectively disrupted with lower applied pressure differences. To maintain sufficient flow in these heat exchangers and achieve the desired heat transfer rate, high fluid velocities need to be obtained by pumping at high pressure. However, large pressure drops make it difficult to maintain such high pressure in fluids. To address this problem, one possible solution is to produce a dynamic deformation of one of the channel walls to create a peristaltic effect that causes the coolant fluid to flow within the heat exchanger at low applied pressure on the fluid domain. This type of heat exchanger is known as dynamic heat exchanger.

Several previous studies have investigated the effects of various parameters on heat transfer in such thermal systems. Billah *et al.* [1] observed that motion and high velocity of the flow through a moving body increased the Nusselt number, leading to higher heat transfer. Rafi *et al.* [2] analyzed the effects of flow velocity (Reynolds number) and channel inclination angle and found that the effect of inclination angle is more prominent at low fluid velocities. Hossain *et al.* [3] studied unsteady fluid flow and heat transfer in a sin wave wavy channel numerically and found steady separation bubbles at the trough of the waves at low velocity. Selimefendigil *et al.* [4] investigated pulsating mixed convection in a multiple vented cavity and found that the minimum Nusselt number values were obtained at the highest frequency due to the system's adaptation to its new flow condition with increasing frequency, leading to decreased heat transfer performance.

Kumar *et al.* [6] and Schmidmayer *et al.* [7] studied heat transfer inside circular sub-millimeter size channels with both static and moving sinusoidal corrugated walls. Fontaine *et al.* [8] studied planar peristaltic pumping devices for CPU cooling. Léal *et al.* [9] presented numerical modeling to determine the fluid flow and thermal performances when one of the channel walls of a heat exchanger was set in continuous motion in a sinusoidal way. The effects of different operating parameters i.e., such as frequency (f), amplitude (A), pressure drop (ΔP), minimum gap between static and dynamic wall (H) and number of crests in the sinusoidal shape (N) of the dynamic wall heat exchanger on the heat transfer performance has not been thoroughly investigated. Numerical analysis involves solving mathematical equations using computational methods. Recently computation fluid dynamics and machine learning have been used to solve different mathematical problems [10]-[12]. In this paper we studied how these different operational parameters influence the heat transfer and pumping performance of the heat exchanger. In addition, streamline and isotherm in different relative amplitude and Oscillation frequency have been investigated which has not been studied before in detail.

II. Physical Modelling

The studied configuration is depicted in Fig. 1a. This configuration represents a steady-state model, and initial values are assumed to be equivalent to the steady-state condition. Using this assumption, the transient model is resolved over a specified time range of 0 to 50/freq, as depicted in Fig. 1b. The proposed system is a channel that is 50 mm × 50 mm × Hmm in size.

Submitted on April 19, 2023.
Published on May 16, 2023.
M. M. Uddin, Northern Illinois University, USA.
(e-mail: mesbahuddin1991@gmail.com)
R. Akhtaruzzaman, The University of Texas at Arlington, USA.
(e-mail: rxa7638@mavs.uta.edu)
T. A. Shanto, The University of Texas at Arlington, USA.
(e-mail: txs5400@mavs.uta.edu)
M. N. Hasan, Assistant professor, BUET, Bangladesh.
(e-mail: nasimme98@gmail.com)

Water flows through this channel, and a constant heat flux of 125 W is applied to the lower wall. The upper wall is dynamically deformed into a sinusoidal waveform. Pressure is maintained at the inlet, and the outlet is thermally insulated without any applied pressure. The dynamic wall is also thermally insulated, and both walls are always subject to a no-slip condition. The ambient temperature is kept constant at T = 27°C.

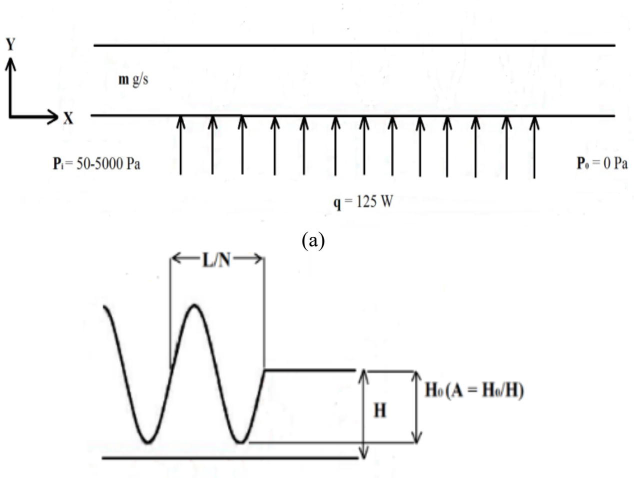

(b)

Fig. 1. a) Schematic diagram of static physical domain; b) wall parameters.

III. Governing Equation

The present investigation employs the continuity, Navier-Stokes, and energy equations to numerically solve for the water domain, utilizing the boundary conditions specified in Table 1. The density is modeled as a function of temperature, and the Boussinesq approximation is implemented, yielding the resultant equations given in (1), (2), and (3).

$$div(\vec{v}) = 0 \tag{1}$$

$$\rho\frac{\partial \vec{v}}{\partial t} + \rho(\vec{v}.\overrightarrow{grad})\vec{v} = \rho\vec{g} - \overrightarrow{grad}(p) + \mu\Delta\vec{v} \tag{2}$$

$$\rho c_p\frac{\partial T}{\partial t} + \rho v\frac{\partial v}{\partial t} + \rho c_p\,\overrightarrow{grad}(T)\vec{v} + \frac{\rho}{2}\overrightarrow{grad}(v^2).\vec{v} = k\Delta T + \frac{\partial p}{\partial t} \tag{3}$$

The solutions for both static and dynamic cases have been determined. The solution for the static case is utilized as the initial values for solving the dynamic case. The equation that governs the displacement of the sinusoidal moving wall includes two smoothing functions or Heaviside functions (denoted as flc^2hs) with two arguments, which are applied to disregard the starting effects of the flow.

The Dynamic wall is governed by (4), (5), and (6).

$$y_{wall} = AYf_X(X)\sin(2\pi(-tf + X\frac{N}{L}))f_t(t) \tag{4}$$

$$f_t(t) = flc2hs(t - \frac{1}{f}, \frac{1}{f}) \tag{5}$$

$$f_X(X) = flc2hs(X - \frac{L}{10}, \frac{L}{20}) * flc2hs(\frac{9L}{10} - X, \frac{L}{20}) \tag{6}$$

The overall heat transfer coefficient, h is defined as (7).

$$h = \frac{q}{\overline{T}_w - \overline{T}_f} \tag{7}$$

IV. Boundary Conditions

The boundary conditions to solve both the static and dynamic case are shown in Table I.

TABLE I: Boundary Conditions

Fluid dynamics condition	Inlet	P = 50 Pa
	Outlet	P = 0 Pa
	Fixed wall	u = v = 0
	Dynamic wall	u = v = 0
Thermal condition	Inlet	T = Tamb = 27 ºC
	Outlet	$\frac{\partial T}{\partial x} = 0$
	Fixed wall	q = 50 000 W/m^2
	Dynamic wall	$\frac{\partial T}{\partial y_{wall}} = 0$

V. Numerical Procedure and Validation

The technique used for solving the governing equation under static conditions is the Galerkin weighted residual method applied to the finite element method. However, for transient conditions, the arbitrary Lagrangian-Eulerian (ALE) method is utilized. A different numerical approach is necessary when the wall undergoes deformation, which results in domain deformation, requiring a freely moving mesh that is compatible with the ALE method. Fig. 2 shows a magnified view of the deformed mesh. To reduce computation time, an extra coarse mesh is used, despite the fact that a finer mesh would yield better accuracy. For the transient case, the time step is selected to be 1/f/20, and the solution is computed for a time duration of 50/f.

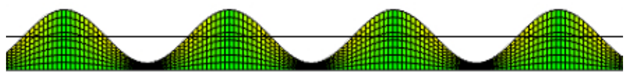

Fig. 2. Magnified image of the deformed mesh at A = 0.9, N = 10, f = 50 Hz and H = 1 mm.

To ensure the accuracy and reliability of the current numerical simulation in solving similar types of problems, a validation process was conducted by comparing the mass flow rate obtained in the present study with that of a previous study by Leal *et al.* [9]. The mass flow rate in kgm^{-2}s^{-1} was calculated by dividing the current paper's mass flow rate by the flow area for various relative amplitude values expressed as a percentage. The results obtained from the present code were then compared with those of Leal *et al.* [9], and it was observed that they closely match, as shown in the Fig. 3 This provides evidence that the current numerical procedure is valid and can be applied to similar types of problems.

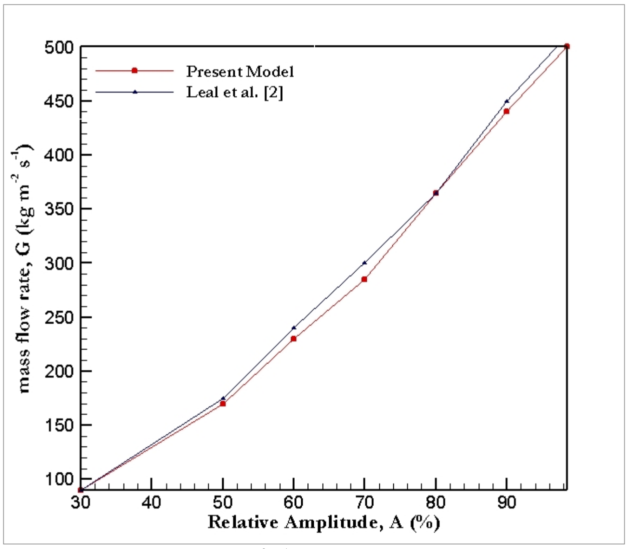

Fig. 3. Comparison of G (kgm^{-2}s^{-1}) vs A(%) graph between present model and that of Leal *et al.* [9].

VI. Results and Discussion

Fig. 4 shows the streamlines for different values of relative amplitude (A) and Oscillation frequency (f) which reveals that when the amplitude is low, the streamlines tend to concentrate at the bottom, resulting in an uneven flow distribution. This phenomenon can be attributed to the denser flow at the bottom, which renders the dynamic wall's impact on the fluid flow insignificant. As the amplitude of dynamic wall deformation increases, the flow becomes more dispersed, leading to a more effective heat transfer. While a change in frequency at lower amplitudes results in a significant shift in the flow pattern, the same alteration at higher amplitudes has no significant effect on the streamlines. Hence, higher amplitude and frequency both improve the flow performance.

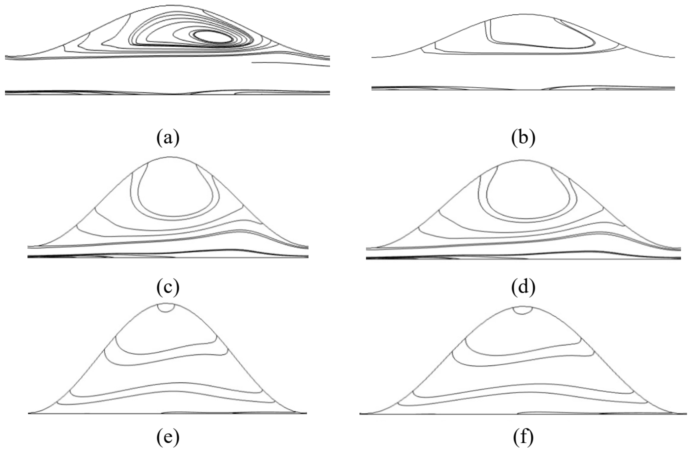

Fig. 4. Streamlines for a) amplitude A= 0.4, f = 25 Hz; b) amplitude A= 0.4, f = 50 HZ; c) amplitude A= 0.6, f = 25HZ; d) amplitude A= 0.6, f = 50 HZ; e) amplitude A= 0.99, f = 25 Hz; f) amplitude A= 0.99, f = 50 Hz, at time, t = 1 sec (N = 10, ΔP = 50 Pa, H =1 mm).

Fig. 5 shows the isotherm for different values of relative amplitude (A) and Oscillation frequency (f). It is clearly visible that at lower amplitudes, the isotherms in a channel with dynamic walls display concentrated heat distribution towards the bottom, indicating uneven thermal behavior. This is due to the reduced impact of dynamic wall effects at lower amplitudes.

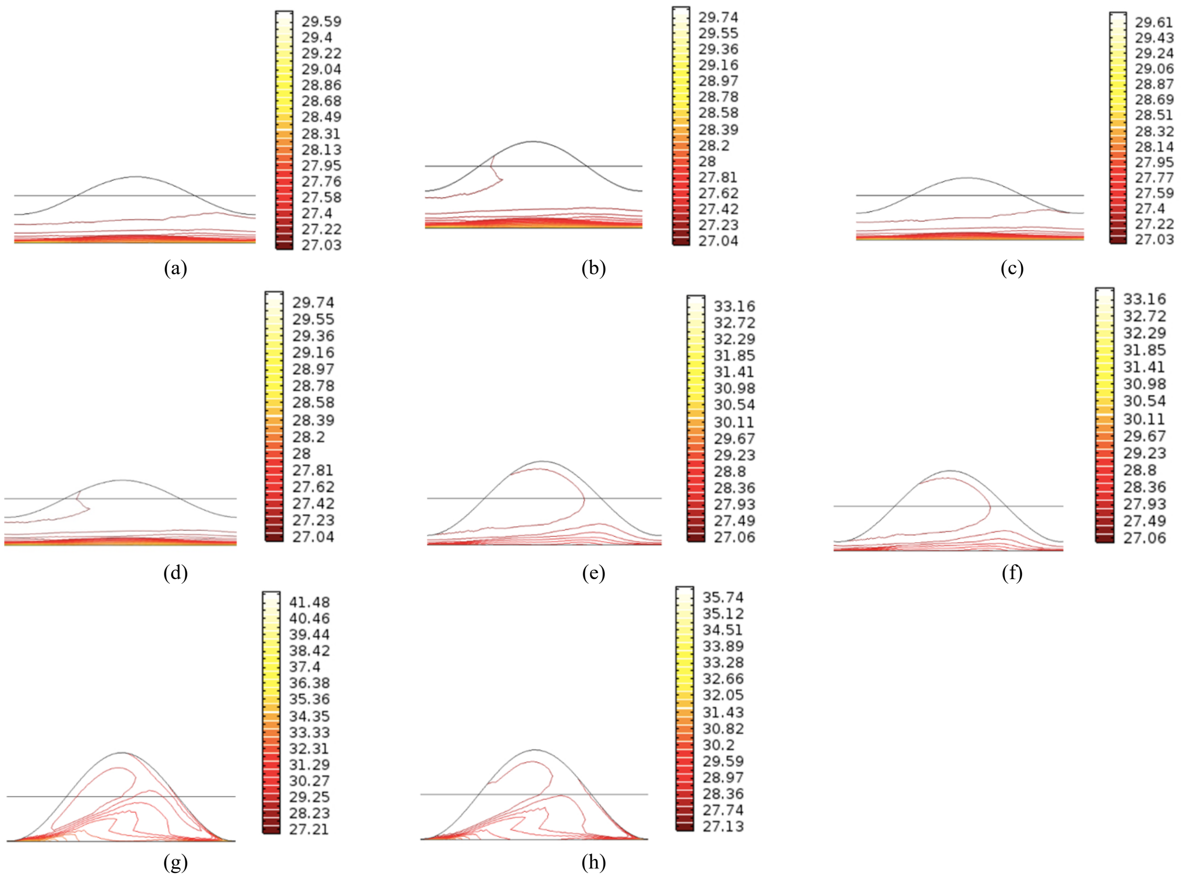

Fig. 5. Isotherms for a) amplitude A= 0.4, f = 25 Hz; b) amplitude A= 0.4, f = 50 HZ; c) amplitude A= 0.6, f = 25HZ; d) amplitude A= 0.6, f = 50 HZ; e) amplitude A= 0.8, f = 25 Hz; f) amplitude A= 0.8, f = 50 Hz; g) amplitude A= 0.99, f = 50 Hz; h) amplitude A= 0.99, f = 50 Hz, at time, t = 1 sec (N = 10, ΔP = 50 Pa, H =1 mm).

However, increasing the amplitude results in more uniform heat distribution across the channel height, making the dynamic wall effects more noticeable. At lower amplitudes, changes in frequency have no discernible effect, whereas, at higher amplitudes, they do.

The alignment between the streamline and isotherm patterns within the heat exchanger indicates a concurrence in the flow behavior and temperature distribution. As the fluid is distributed with higher amplitude, there is greater uniformity in the heat transfer process. Enhanced heat and mass transfer are observed at higher amplitudes and frequencies, with the optimum performance observed at a relative amplitude of 99% and a frequency of 50 Hz.

Fig. 6 depicts the relationship between mass flow rate and relative amplitude. The graph indicates that as the amplitude of the wall motion increases, the mass flow rate also increases. This phenomenon occurs because the flow in the dynamic wall heat exchanger is not solely driven by the pressure difference, but also by the wave of deformation induced by the motion of the wall. This sinusoidal movement of the wall causes a peristaltic action that pumps a greater volume of fluid through the gap, leading to an increase in the mass flow rate as the amplitude of the wall motion increases. Furthermore, for a given amplitude, the mass flow rate is greater when the channel height (H) is increased. However, the increase in flow rate does not vary with amplitude, as indicated by the parallel lines in Fig. 6. This increase in mass flow rate is a result of the increase in inlet areas with higher channel height, whereas amplitude does not have an additional effect on this height.

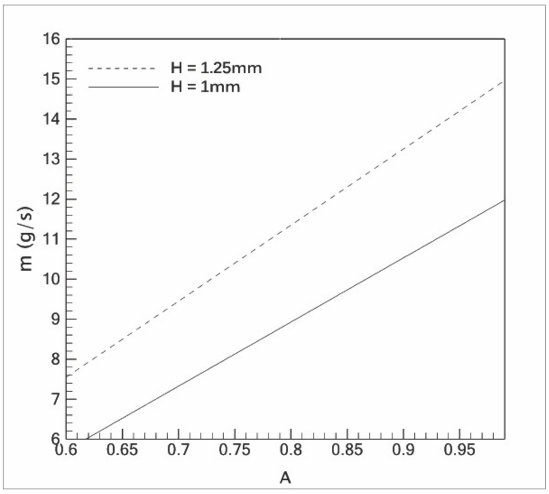

Fig. 6. Mass flow rate, m vs relative amplitude, A (N=10, f=50Hz, ΔP=50Pa).

The height of the dynamic wall is varied and that variation in the height of a dynamic wall causes an increase in the extent of variation as the amplitude increases, resulting in greater mixing. The troughs between two waves experience mixing, and the highest heat transfer occurs at the trough where thermal resistance is lowest, owing to the decrease in the fluid domain between the heat flux and dynamic wall.

At higher amplitudes, the lowest point becomes closer to the fixed wall, resulting in a higher heat transfer coefficient, as evidenced by both Fig. 7 and Fig. 8.

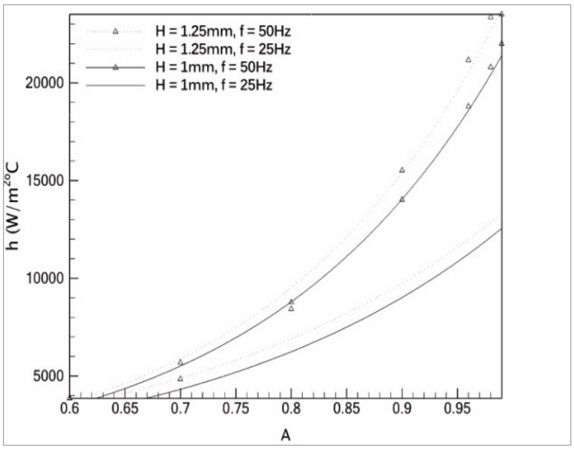

Fig. 7. Heat transfer coefficient, h vs relative amplitude, A (N=10, ΔP=50Pa).

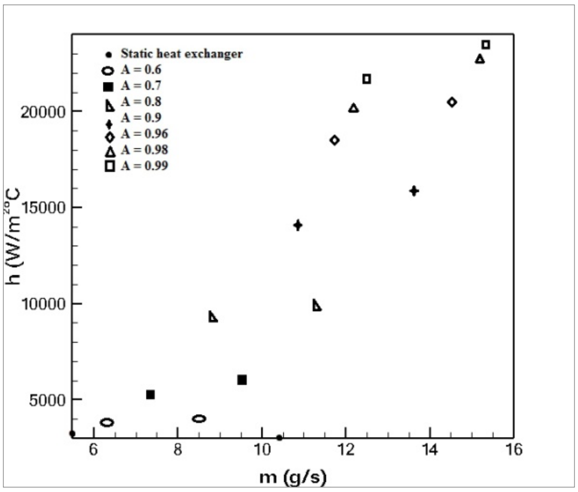

Fig. 8. Heat transfer coefficient, h vs mass flow rate, m (N=10, ΔP=50Pa).

Fig. 7 reveals that, at the same amplitude, a dynamic wall moving at a higher frequency exhibits a higher heat transfer coefficient. This is anticipated, as more peristaltic motions of the wall lead to increased mixing. Moreover, Fig. 8 indicates a slight increase in the heat transfer coefficient when channel height is raised, owing to a greater mass flow rate and resulting mixing. However, the heat transfer increase at the same relative amplitude is very minor. Therefore, increasing the channel height does not contribute significantly to the enhancement of the heat transfer coefficient.

As the frequency of waves increases, the wavelength decreases, resulting in a smaller volume of fluid between each pair of troughs, albeit with a marginal change. According to Fig. 9, a decrease in wavelength (N = 10) leads to a slightly higher decline in heat transfer coefficient at lower relative amplitude, whereas higher wavelength (N = 8) results in greater heat transfer. This trend is reversed at very high relative amplitude. Between the range of 0.85 < A < 0.9, all three analyzed wavelengths exhibit the same outcome. Since N = 10 displays less variation with relative amplitude, it is recommended as the optimal performance parameter.

The flow in a given domain is driven by two factors: the pressure difference in the direction of the flow and the pumping action induced by the dynamic wall. Consequently, a small pressure differential is sufficient to achieve the desired flow rate and the desired heat transfer performance.

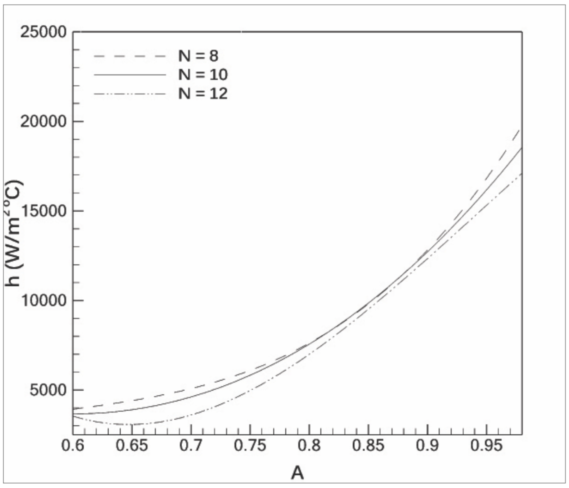

Fig. 9. Heat transfer coefficient, h vs relative amplitude, A (f=50Hz, h=1mm, ΔP=50Pa).

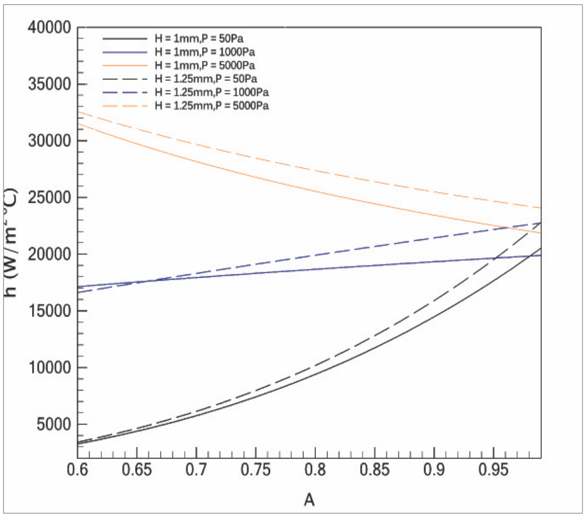

Fig. 10. Heat transfer coefficient, h vs relative amplitude, A (f=50Hz, N=10).

As illustrated in Fig. 10, regardless of the magnitude of the externally applied pressure difference, the heat transfer remains constant at higher amplitudes. This stands in contrast to a static wall, where the pressure difference serves as the sole driving force and an increase in heat transfer is expected with increasing pressure. Therefore, the primary advantage of a dynamic wall heat exchanger is its ability to achieve very high heat transfer coefficients with a small pressure difference.

VII. Conclusion

This paper focuses on investigating the impact of various parameters on the performance of a recently introduced heat exchanger, known as the dynamic heat exchanger. Specifically, the study analyzed the effects of the amplitude, number of waves per unit length, and frequency of oscillation of the dynamic wall, as well as the externally applied pressure on the fluid domain. Finally, the following conclusion is drawn about the optimum performance parameters:

1) Mixing intensification takes place at higher amplitudes owing to the prominent performance of the dynamic wall.
2) A higher frequency results in an accelerated peristaltic action of the dynamic wall, thereby augmenting heat transfer.
3) Opting for a smaller height channel is preferable due to a marginal improvement in performance beyond a certain channel height, and because of the desire for a compact heat exchanger.
4) As the dynamic wall motion induces flow, a minor pressure difference is adequate to achieve a high heat transfer coefficient.

Acknowledgment

We express our gratitude to the Department of Mechanical Engineering at Bangladesh University of Engineering and Technology (BUET) for their unwavering support and constant encouragement during our research efforts.

References

[1] Billah MM, Khan MI, Rahman MM, Alam M, Saha S, Hasan MN. *Numerical study of mixed convection heat transfer enhancement in a channel with active flow modulation*; 2017. doi: 10.1063/1.4984733.

[2] Rafi AA, Tonmoy MTA, Hasan MN. *Numerical study of mixed convection heat transfer in an inclined rectangular channel with extruding discrete multiple heaters*; 2016. doi:10.1063/1.4958430.

[3] Hossain MZ, Islam AKMS. Fully developed flow structures and heat transfer in sine-shaped wavy channels. *Int. Comm. Heat Mas Transfer;* 2004;31(6):887-896.

[4] Selimefendigil F, Öztop HF. Numerical investigation and dynamical analysis of mixed convection in a vented cavity with pulsating flow. *Computers & Fluids*. 2014; 91: 57–67. doi:10.1016/j.compfluid.2013.11.033.

[5] Rabie LH, Mostafa HM. An Experimental Study for Heat Transfer In Laminar Pulsating Annular Flow. *Mansoura Engineering Journal (MEJ)*. 2001;26(2):M54-M65.

[6] [Kumar P, Schmidmayer K, Topin F, Miscevic M. Heat transfer enhancement by dynamic corrugated heat exchanger wall: Numerical study. *Journal of Physics: Conference Series*. 2016; 745: 032061. doi:10.1088/1742-6596/745/3/032061.

[7] Schmidmayer K, Kumar P, Lavieille P, Miscevic M, Topin F. Thermo-hydraulic characterization of a self-pumping corrugated wall heat exchanger. *Energy*. 2017; 128: 713–728. doi:10.1016/j.energy.2017.04.048.

[8] Fontaine JM, Pigache F, Miscevic M, Rouchon J-F, Topin F. Studying impacts of travelling wave shape on pumping for active cooling. *IEEE International Workshop of Electronics, Control, Measurement, Signals and Their Application to Mechatronics (ECMSM)*. 2017. doi:10.1109/ecmsm.2017.7945863.

[9] Léal L, Topin F, Lavieille P, Tadrist L, Miscevic M. *Simultaneous integration, control and enhancement of both fluid flow and heat transfer in small scale heat exchangers: A numerical study.* International Communication of Heat and Mass Transfer. 2013;49:36-40.

[10] Ahamed S, Uddin MM. *Estimating uncertainty of earthquake rupture using Bayesian neural network.* Physics Stat. 2019. Retrieved from: arXiv.org. https://arxiv.org/abs/1911.09660v2.

[11] Uddin MM. Finite Difference Analysis of Stress Distribution Around an Elliptical Hole in a Plate Subjected to Axial Loading. *International Journal of Modern Developments in Engineering and Science*. 2023;2(4):1-4. https://journal.ijmdes.com/ijmdes/article/view/119.

[12] Uddin MM. Studying the Scratching Behavior of Nb/Nbc Nanolaminate Using Molecular Dynamics Atomistic Simulations. Northern Illinois University. ProQuest Dissertations Publishing; 2020.

[13] Uddin MM. Study the effect of different ellipse sizes on the stress distribution around an elliptical hole in a plate subjected to axial loading using Finite difference analysis. *IOSR Journal of Mechanical and Civil Engineering (IOSR-JMCE)*. 2023 Mar-Apr;20(2 Ser. III):37-41. doi: 10.9790/1684-2002034257.

[14] Uddin MM. *Study the effect of scratching depth and ceramic-metal ratio on the scratch behavior of NbC/Nb Ceramic/Metal nano-laminates using molecular dynamics simulation and machine learning*. arXiv:2305.03698v1 [cond-mat.mtrl-sci]. 2019 May. [Internet]. Available from: https://doi.org/10.48550/arXiv.2305.03698.